Prediction of the Small-*k* Behavior of the Structure Factor ($S(k)$) for Rubidium and Cesium via a New Model for the Direct Correlation Function and Evaluation of Some Reported Effective Pair Potentials

Ezat Keshavarzi* and Mohammad Kamalvand

Department of Chemistry, Isfahan University of Technology, Isfahan, Iran

Received: October 5, 2003; In Final Form: April 20, 2004

In this article, we have used a newly presented direct correlation function (DCF) and predicted the small-*k* behavior of the structure factor, $S(k)$, for liquid rubidium and cesium, and this behavior is in very good agreement with the experimental data. For these calculations, the effective pair potentials have obtained using the modified hyper-netted-chain (MHNC) theory. These effective pair potentials are also accurate for the range in which no pseudopotential, or Lennard-Jones (LJ) potential, is adequate to present the thermodynamic behavior of alkali metals. We have also compared our model with the Percus−Yevick theory and random phase approximation in regard to predicting $S(k)$ at low k, and a better agreement has been obtained. Because the applied model for the DCF generates $S(k)$ accurately at low k, we have used it to evaluate some reported effective pair potentials for alkali metals, including LJ ($n-m$) and also exp-6 types. The results show that these potentials are not very accurate, at least for the moderate densities, in regard to predicting $S(k)$, although these potentials are able to generate the pressure−volume−temperature ($p-v-T$) behavior of alkali metals precisely.

1. Introduction

Alkali metals, in comparison with normal fluids, do not follow the law of corresponding states,[1] in which interactions between particles at the solid, liquid, and gaseous phases are supposed to have the same form. In fact, the interatomic interactions in these fluids are strongly dependent on the thermodynamic state of the system.[1] For example, the structure of a solid metal is usually considered to be a collection of ions, fixed in a solid matrix, thus creating an ionic lattice. Therefore, valence electrons are delocalized over the lattice and, hence, have little correlation with core electrons.[2] Therefore, ion−ion, electron−ion, and electron−electron interactions exist in the system. For liquid densities near the melting point, the interatomic pair potentials of alkali metals are the same as those in solid state and may be described by the pseudopotential obtained from first-order perturbation theory based on the nearly free electron (NFE) model.[1] This potential consists of a direct coulomb potential (repulsion) between the ions, plus the attraction of each ion to the screening charge distribution induced by the pseudopotential of the second ion.[3,4] This effective pair potential describes the interatomic potential and structure of the metals with relativity high accuracy only when the density of fluid is more than twice the critical density.[5]

For lower densities, the free electrons belong to its ions and, thus, the NFE model fails to give a reasonable pair potential, especially near the critical point. In these states, alkali-metal fluids consist of neutral atoms, molecules, and some small clusters, and the interaction potentials between these atoms and molecules may be described, in some cases, by a simple potential without an oscillating tail.[6,7] However, up to now, there has not been any report for the reliable interatomic pair potential, derived theoretically, that is able to describe the behavior (and also the structure) of the system in these states accurately.[6]

With further decreasing density in the gaseous phase, the fluid is in an atomic form and interactions between these atoms are van der Waals forces and may be considered as the LJ-type pair potential.[6]

In fact, the interatomic interactions for alkali metals change from a screened columbic potential to LJ-type interactions with decreasing density. Therefore, the interatomic interactions at moderate densities are very complex and there is no theoretical method to obtain them. Fortunately, studies on the experimental structure factor, $S(k)$, of alkali metals provides an important source of information for the interatomic interactions. The structure factor at low k is very sensitive to the intermolecular interactions at the long-range limit,[8] including the oscillatory repulsive forces, whereas the short-range potential has a central role in the large values of k.[9] Two main approaches to get the intermolecular interactions from the experimental $S(k)$ exist, and they are as follows:

(1) The integral equations, including the Percus−Yevick (PY), hyper-netted-chain (HNC), and modified hyper-netted-chain (MHNC) equations. The MHNC method is more accurate, in comparison with the others, in regard to predicting the pair potential[9] of a fluid; however, this theory fails at high temperatures.[10] Accurate effective pair potentials have been obtained for some states of Rb[7] and Cs[6] via this method in which the oscillatory form of the potential, and also its dependency on density, may be observed. These potentials are in a qualitative agreement with the pseudopotentials at high density; however, when the NFE model breaks down, this agreement fails.[7]

(2) Perturbation theories, such as the Weeks−Chandler−Andersen[11] (WCA) approach, random phase approximation (RPA),[12] and optimized random phase approximation (ORPA).[3]

* Author to whom correspondence should be addressed. Fax: +98-311-3912350. E-mail address: keshavrz@cc.iut.ac.ir.

10.1021/jp0369802 CCC: $27.50
Published on Web 06/29/2004

In this article, we have predicted the low-angle structure factor for rubidium and cesium, using the newly presented direct correlation function (DCF).[13] In our procedure, the required effective pair potential was obtained using the MHNC method.[6,7] We have also compared our results with some known theories, such as PY and RPA. Because $S(k)$ is produced accurately using this model, we decided to evaluate some effective pair potentials (including LJ ($n-m$) types, from ref 2) and also exp-6 types, from ref 1) that have been able to present the pressure−volume−temperature ($p-v-T$) behavior of fluids precisely. Initially, we explain our DCF model and also the procedure for prediction of $S(k)$ in the following sections.

2. Prediction of Low-k Behavior of the Structure Factor $S(k)$ for Alkali Metals

The potential energy of monatomic fluid may be assumed by a sum of pairwise potentials $\varphi(r)$. Based on the perturbation approach, $\varphi(r)$ is divided into a reference component ($\varphi_0(r)$) and a perturbation component ($\varphi_1(r)$):

$$\varphi(r) = \varphi_0(r) + \varphi_1(r) \tag{1}$$

Following the Weeks−Chandler−Andersen (WCA) theory,[11] the reference component (the core potential) and the perturbation component (the remaining attractive force portion of the potential) may be written as

$$\varphi_0(r) = \begin{bmatrix} \varphi(r) - \varphi(r_0) & (\text{for } r < r_0) \\ 0 & (\text{for } r \geq r_0) \end{bmatrix} \tag{2}$$

$$\varphi_1(r) = \begin{bmatrix} \varphi(r_0) & (\text{for } r < r_0) \\ \varphi(r) & (\text{for } r \geq r_0) \end{bmatrix} \tag{3}$$

where $\varphi(r_0)$ is the first minimum of $\phi(r)$. In the same manner as potential, we may divide[13] the DCF into two contributions:

$$c(r) = c_0(r) + c_1(r) \tag{4}$$

in which the first term, $c_0(r)$, is the DCF of the reference system and other term, $c_1(r)$, is a perturbation component. According to ORPA,[14] we consider $c_0(r)$ via a summation of $c_{hs}(r)$, which is the DCF of the hard-sphere fluid at the same temperature and density, and the "blip" function, $B(r)$:

$$c_0(r) \cong c_{hs}(r) + B(r) \tag{5}$$

where

$$B(r) = y_{hs}(r)[\exp(-\beta\varphi_0(r)) - \exp(-\beta\varphi_{hs}(r))] \tag{6}$$

with

$$y_{hs}(r) = \exp(\beta\varphi_{hs}(r))g_{hs}(r) \tag{7}$$

where $\beta = 1/(kT)$ has its usual meaning, $g_{hs}(r)$ is the hard-sphere radial distribution function, and $\varphi_{hs}(r)$ is its pair potential. In the WCA theory, the hard-sphere diameter, d, is determined at each temperature and density by the following requirement:[11]

$$B(k=0) = \int B(r) r^2 \, dr = 0 \tag{8}$$

$B(r)$ or $B(k)$, which is the Fourier transform of $B(r)$, takes into account the softness of the repulsive potential, in which the higher-order contributions from $B(k)$ are neglected in the low-k region. Therefore, we have

$$c_0(r) = \begin{bmatrix} c_{hs}(r) & (\text{for } r < d) \\ 0 & (\text{for } r \geq d) \end{bmatrix} \tag{9}$$

The PY expression has been used for $c_{hs}(r)$:

$$c_{hs}(r) = \begin{bmatrix} -a - b(r/d) - c(r/d)^3 & (\text{for } r < d) \\ 0 & (\text{for } r \geq d) \end{bmatrix} \tag{10}$$

and the coefficients are given by

$$a = \frac{(1+2\eta)^2}{(1-\eta)^4}$$

$$b = -6\eta\frac{(1+\eta/2)^2}{(1-\eta)^4}$$

$$c = \frac{a\eta}{2} \tag{11}$$

where η is the packing fraction ($\eta = \pi\rho d^3/6$) and ρ is the number density.

It is interesting to seek a modification of ORPA that maintains the simplicity of the original formulation, while accounting more accurately for the effects of nonlinear interactions in $c(r)$. Therefore, we assumed that $c_1(r)$ is related to the attractive interactions, $\varphi_1(r)$, in a nonlinear form:[13]

$$c_1(r) = \exp(-\beta\phi_1(r)) - 1 \tag{12}$$

In this way, the second virial coefficient, near the critical temperature (T_c), is not very dependent on the specific form of the interactions and gives a universal value that is similar to the simulation results.[10,15] The second reason for choosing $c_1(r)$ to be represented by eq 12 is the experimental evidence. The experimental results show that the DCF has a negative component for $r < \sigma$ (where σ is the molecular diameter) and rises steeply at $r \approx \sigma$, and then looks very similar to the Mayer-f function, although it is somewhat smaller. In fact, the tail of $c(r)$ decreases as temperature increases, and, at very high temperatures, the core of $c(r)$ has dominated.[16−18] It is also known that the Ornstein−Zernike (O−Z) function, which relates the DCF to the pair distribution function, reduces to a simple expression at low density:[16]

$$g(r) - 1 = c(r) = \exp(-\beta\phi(r)) - 1 \qquad (\text{for } \rho \to 0) \tag{13}$$

Of course, at very high temperatures, the exponential term of eq 13 may be expanded as[17]

$$\exp(-\beta\phi(r)) = 1 - \beta\phi(r) + \ldots \tag{14}$$

and then

$$c_1(r) = -\beta\phi_1(r) \tag{15}$$

which is the same analytical expansion for the tail of $c(r)$ in ORPA.[14] We used such an equation (eq 13) for higher densities, by means of an effective pair potential.[13,17] On the other hand, we accounted for the contribution of many-body interactions in the effective pair interatomic potential. Using eqs 9 and 12, the overall expression for the DCF in our model is[13]

$$c(r) = c_{hs}(r) + \exp(-\beta\phi_{eff_1}(r)) - 1 \tag{16}$$

In all calculations, we first should have the effective pair potentials and d_{eff}, which are dependent on T and ρ. The

TABLE 1: Potential Parameters (Including r_0, the Position of Minimum of Potential) for Rb[22] and Cs[6]

No.	substance	temperature, T (K)	ρ (g/cm^3)	r_0 (Å)	$\varphi(r_0)/k$ (K)	$S(0)$	d (Å) from eq 8	d (Å) from eq 17
1	Rb	2000	0.540	5.04	414.08	3.51[a]		3.372
2	Rb	1700	0.798	5.13	814.81	0.98[a]	4.082	4.016
3	Rb	1400	0.970	5.23	777.14	0.40[a]	4.205	4.249
4	Rb	900	1.214	5.32	448.11	0.12[a]	4.204	4.329
5	Rb	350	1.459	5.11	570.75	0.02[a]	4.603	4.333
6	Cs	1673	0.762	5.95	362.04	0.86[b]	4.028	
7	Cs	1373	1.210	5.93	536.43	0.41[b]	4.377	
8	Cs	773	1.570	5.74	264.44	0.072[b]	4.563	

[a] From ref 19. [b] From ref 6.

effective pair potential has been extracted for alkali metals from MHNC theory. To obtain d_{eff}, we may use the reduced bulk modulus, as follows:

$$Br = \frac{1}{S(0)} = \frac{1}{k_B T}\left(\frac{\partial p}{\partial \rho}\right)_T = 1 - 4\pi\rho \int c(r) r^2 \, dr \qquad (17)$$

where Br may be calculated from the $p-v-T$ data. We can also use the blip function (eq 8) to obtain d_{eff}.

To predict $S(k)$ for small k at different thermodynamic states, we obtain $c(k)$,

$$c(k) = 4\pi \int c(r) \frac{\sin(kr)}{kr} r^2 \, dr \qquad (18)$$

and then calculate the structure factor $S(k)$ via the following equation:

$$S(k) = \frac{1}{1 - \rho c(k)} \qquad (19)$$

It is clear that all approximations that have been used in our model may be exaggerated in the Fourier transform. Therefore, we have investigated the accuracy of the model via the prediction of the low-k behavior of $S(k)$.[13] As we mentioned, the effective pair potentials have been extracted from experimental pair distribution function and MHNC theory[6,7] numerically. In this way, $\varphi(r_0)$, using the numerical effective pair potential, has been chosen as the first minimum value of the effective pair potential. Therefore, the only undetermined parameter in eq 4 is d_{eff}, which may be obtained from either eq 8 or eq 17. We have calculated the value of d from eq 8 and also eq 17 separately and observed that the obtained values for d_{eff} are different from each other (by up to 6.2%, which is not a very serious error) (see Table 1). For several states, we could not get a value for d using eq 8 for cesium. The effective pair potential in cesium is softer, in comparison to the LJ potential; therefore, the range in which $B(r)$ has a negative value may be increased, so that eq 8 does not give any acceptable value for d_{eff}. Therefore, we suggest using eq 17 to obtain the value of d_{eff} in any thermodynamic state. We have also omitted $B(r)$ from eq 5, because it is so small, and we also may soften $c(r)$ for $r < r_0$ by $\exp(-\beta\varphi_{\text{eff}}(r_0))$. For any thermodynamic states, the DCF function then has been calculated using the values of $\varphi(r_0)$ and d_{eff}.

3. Results and Discussion

3.1. Comparison of the Calculated $S(k)$ at Low k with the Experimental Data, PY and RPA Theories for Rubidium and Cesium. We have used the experimental effective pair potentials for some thermodynamic states of rubidium[7] and cesium,[6] obtained by MHNC theory and the new model for the DCF, and then predicted the small-k behavior of $S(k)$. In Figure 1, we have presented the low-k behavior of $S(k)$ for rubidium at 1700 K and a density of 0.798 g/cm^3 and compared this behavior with experimental data. According to our calculation, $d_{\text{eff}} = 4.082$ Å and value of $\phi(r_0)$ has been obtained from the experimental effective pair potential[7] as $\phi(r_0)/k = 814.81$ K. As Figure 1 clearly shows, excellent agreement is observed between the experimental results and our predictions. We have also performed similar calculations for the other states of rubidium and cesium; their results are summarized in Figures 1 and 2. In Table 1, the calculated values for the hard sphere diameter (d_{eff}), effective pair potential well depth, and other required information for these thermodynamic states have been presented.

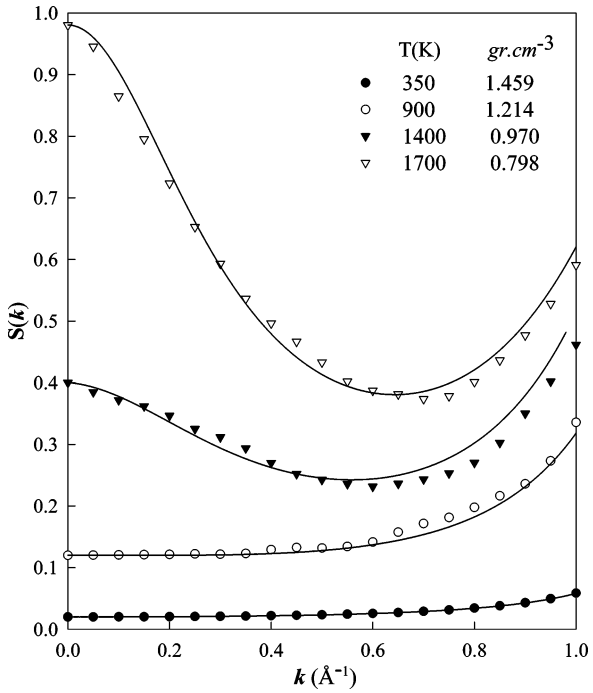

Figure 1. Calculated structure factor for rubidium obtained using the new model for the DCF and the experimental effective pair potential (solid lines), compared with the experimental structure factor from ref 22 (symbols).

Comparison between our calculations with their corresponding experimental values shows very good agreement for rubidium. For all the examined states of rubidium, for which the density is greater than the density of the metal−nonmetal transition[20] (M−NMT) (for rubidium, $\rho_{\text{M-NMT}} = 0.69$ g/cm^3), $S(k)$ has been generated very precisely, in comparison with experimental data. Except $S(k)$ cannot be generated by our model for DCF at $T = 2000$ K ($\rho = 0.54$ g/cm^3). We

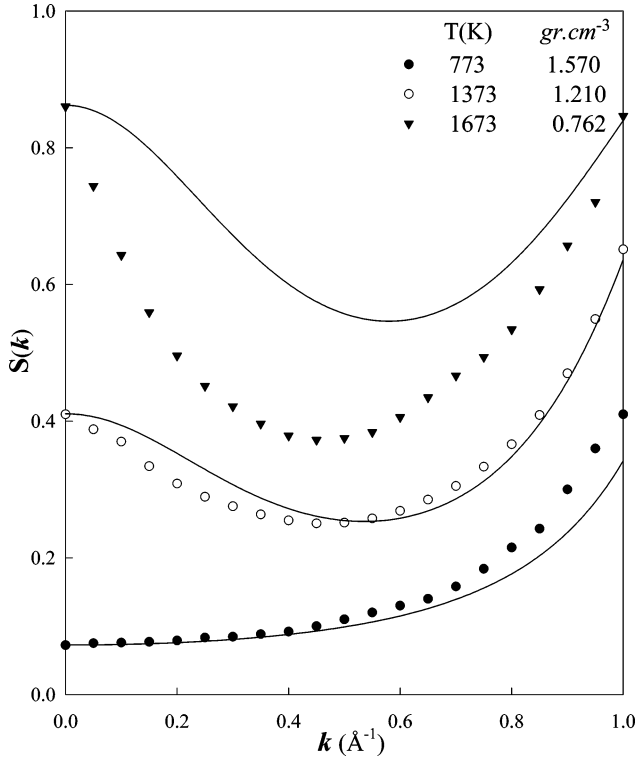

Figure 2. Calculated structure factor for cesium obtained using the new model for the DCF and the experimental effective pair potential (solid lines), compared with the experimental structure factor from ref 6 (symbols).

know that this state is close to the critical point and that its experimental structure factor is rather scattered and there is some uncertainty on these data;[7] on the other hand, the MHNC method failed to obtain good values for the effective pair potential at high temperatures.[10] Therefore, this failure in the prediction of $S(k)$ may be expected. In addition, the density of this state is also lower than the M−NMT density. The deviation of the calculated structure factor from the experimental data observed only in state 6 of Table 1 for cesium. Note that the density of this thermodynamic state is noticeably lower than the M−NMT density (for Cs, $\rho_{\mathrm{M-NMT}} = 1.2$ g/cm^3) and maybe this failure is due to this fact.

For evaluation of our theory in prediction of the structure factor, we compared our results with the PY and RPA theories. To obtain the results of the RPA theory, we have calculated the structure factor of rubidium using d_{eff} that was obtained using eq 8. The results of the PY theory have been taken from ref 21. The results have been summarized in Figure 3 for two mentioned states. We have also performed the same comparison for the other states of rubidium, and similar results have been obtained. In this way, we may conclude that our model in prediction of structure factor is more successful in comparison with some known theories.[13]

In this way, we may conclude that our model is applicable for alkali metals with some modifications. Because the efficiency of our DCF model has improved using the experimental data, we can use this model to evaluate some approximated pair potentials, which is claimed as the effective pair potential of alkali metals in the following section.

3.2. Evaluation of the Effective Pair Potentials for Alkali Metals. Recently, a new equation of state (EOS), the linear isothermal regularity[19] (LIR), has been derived for dense fluids. The derivation of the LIR starts with the exact thermo-

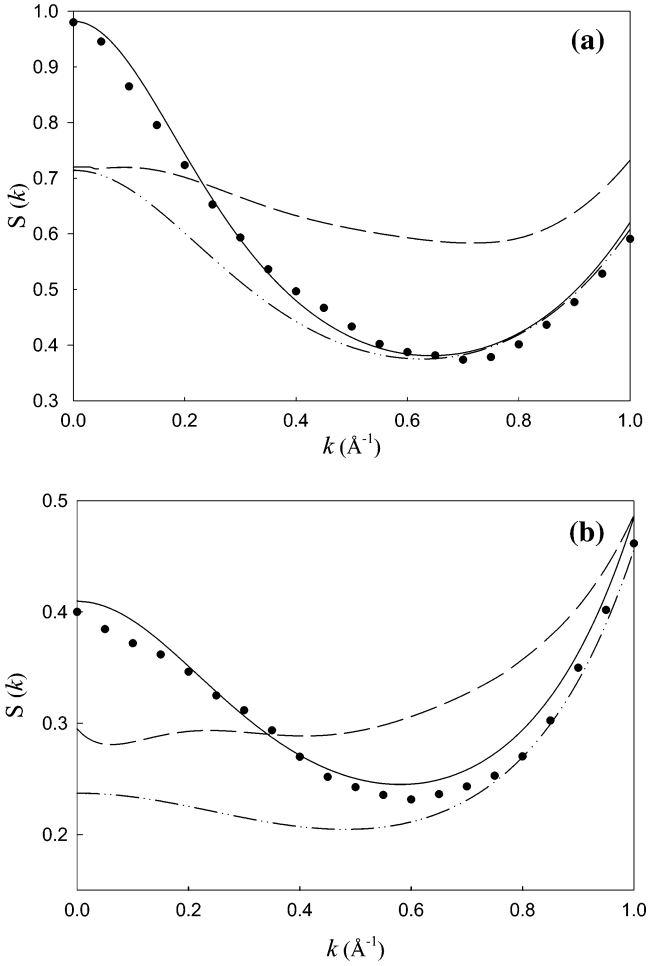

Figure 3. Comparison of the calculated structure factor for rubidium obtained using the new model (—) for the DCF ((a) $\rho = 0.798$ g/cm^3 and $T = 1700$ K, and (b) $\rho = 0.970$ g/cm^3 and $T = 1400$ K); (−••−) RPA and (− −) PY results (ref 21) are also shown. The experimental structure factor (data denoted by a solid circle, ●) has been reported from ref 22.

dynamic relation for pressure, p:

$$p = T\left(\frac{\partial p}{\partial T}\right)_{\rho} - \left(\frac{\partial E}{\partial V}\right)_{T} \tag{20}$$

where E is the internal energy. Parsafar and Mason[19] assumed that $(\partial E/\partial V)_T = (\partial U/\partial V)_T$, where U is the average potential energy, which is approximated by summing the contribution from the nearest neighbors only, assuming single inverse power for the effective repulsion and attraction. In this way, the average potential energy among N molecules is obtained by

$$U = \frac{N}{2} z(\rho) \varphi_{\mathrm{eff}}(\bar{r}) \tag{21}$$

where $z(\rho)$ is the average number of nearest neighbors and

$$\varphi_{\mathrm{eff}}(\bar{r}) = \frac{C_n}{\bar{r}^n} - \frac{C_m}{\bar{r}^m} \tag{22}$$

where $\bar{r}$ is the average distance between nearest neighbors, and C_n and C_m are constants. The function $z(\rho)$ is taken to be proportional to ρ, and $1/\rho = \bar{r}^3$; therefore, U can be written as

$$\frac{U}{N} = \frac{K_n}{v^{(n/3)+1}} - \frac{K_m}{v^{(m/3)+1}} \tag{23}$$

where K_n and K_m are constants and υ is the molar volume. After performing the differentiation, the internal pressure can be described by[19]

$$p_{\text{int}} = \left(\frac{\partial E}{\partial \upsilon}\right)_T \cong \left[\frac{\partial (U/N)}{\partial \upsilon}\right]_T = A_1 \rho^{(m/3)+2} - B_1 \rho^{(n/3)+2} \quad (24)$$

where A_1 and B_1 are constants. Combining eqs 20 and 23 gives

$$(Z-1)\upsilon^2 = -\frac{A_1}{RT}\rho^{(m/3)-1} + \frac{B_1}{RT}\rho^{(n/3)-1} + \frac{1}{\rho^2}\left[\frac{1}{\rho R}\left(\frac{\partial p}{\partial T}\right)_\rho - 1\right] \quad (25)$$

where $Z = p\upsilon/(RT)$. The last term in eq 24 is replaced by a constant, A_2. In this model, $m = 3$ and $n = 9$ (according to the LJ (12−6) potential) and the final result is, therefore, of the form[19]

$$(Z-1)\upsilon^2 = A + B\rho^2 \quad (26)$$

where $A = A_2 - A_1/(RT)$ and $B = B_1/(RT)$. According to the LIR, $(Z-1)\upsilon^2$ is linear versus ρ^2 for any isotherm when $\rho > \rho_B$ and $T < 2T_B$ (ρ_B and T_B are the Boyle density and temperature, respectively). In our previous work,[20] we examined the LIR-EOS for prediction of the $p-\upsilon-T$ behavior of alkali metals; we have observed that this regularity also holds for alkali metals when they are in the metallic states ($\rho > \rho_{M-NMT}$). We have performed some modifications on the LIR-EOS[20] and used it for nonmetallic states too. According to the LIR derivation, in two separate papers, the exp-6 and the LJ (6−3) effective pair potentials (from refs 1 and 2, respectively) have been used in the LIR derivation instead of the LJ (12−6) potential and obtained two EOSs for these metals. By considering the exp-6 and LJ (6−3) potentials in the LIR derivation as the effective pair potential, they have determined that the isotherm of $(Z-1)\upsilon^2$ is linear versus $\rho^{-7/3}\exp\{\alpha[1-(C\rho^{-1/3}/r_m)]\}$ (from ref 1) and $1/\rho$ (from ref 2), respectively, for liquid cesium for wide range of thermodynamic states from melting to the critical point, where C and α are constants and r_m is the minimum position of potential. We have evaluated these mentioned potentials for alkali metals by applying them in our model in the DCF and calculated the low-k behavior of structure factor. For this purpose, we have used the reported values for ϵ_{eff}, r_m, and σ_{eff} for the LJ (6−3) and exp-6 models from refs 1 and 2 in our DCF for any thermodynamic states. Our results show that we cannot obtain any values for hard diameter at low temperature using the exp-6 potential from eq 8 or eq 17 separately and for temperatures that it is possible to calculate a value for d_{eff}; the obtained $S(k)$ value does not have any acceptable form. Also, we repeated these calculations for the LJ (6−3) potential (which is applied in the LIR EOS) and observed that, for temperatures for which it is possible to calculate values for d, we cannot generate general form of $S(k)$ versus k. Figure 4 shows some of these typical results. The figure clearly shows that the deviation is considerable, and, in some cases, we cannot generate the acceptable values for $S(k)$. In this way, we may say that these effective pair potentials may not be considered as the effective pair potential for alkali metals, at least to predict $S(k)$. This conclusion may be also confirmed by comparing these effective pair potentials with some states for which we have the MHNC calculations, which have bumping (in these potentials, no bumping has been predicted).

Moreover, we have also examined some LJ ($n-m$) potentials for rubidium in the DCF model to generate the $S(k)$ at low k.

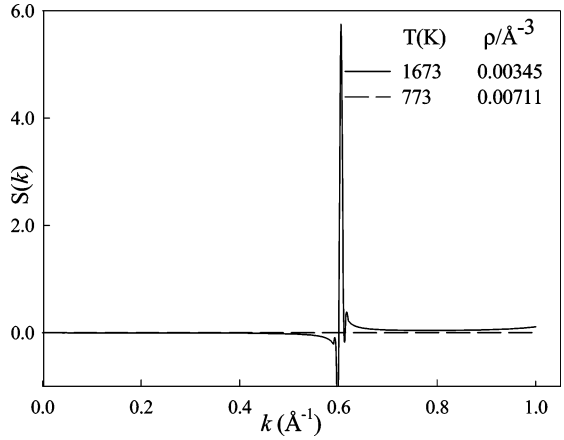

Figure 4. Prediction of structure factors using the LJ (6−3) potential (used in the linear isothermal regularity (LIR), similar to the equation of state (EOS)) for cesium, for two cited thermodynamic states.

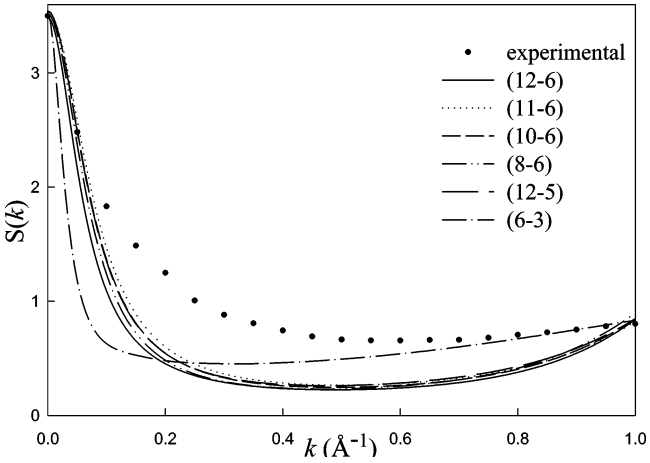

Figure 5. Calculated structure factors ($S(k)$) using various LJ ($n-m$) potentials and a new model for DCF for rubidium at $T = 2000$ K and $\rho = 0.54$ g/cm^3.

TABLE 2: Potential Parameters for a Lennard-Jones (LJ) ($n-m$) Potential Using the Experimental Second Virial Coeffcient

No.	substance	LJ potential ($n-m$)	σ (Å)	ϵ/k (K)
1	Rb	12−6	5.2	1650
2	Rb	11−6	5.05	1620
3	Rb	10−6	5.1	1580
4	Rb	8−6	5.15	1500
5	Rb	12−5	5.1	1550
6	Rb	12−4	5.05	1430
7	Rb	12−3	5.0	1100
8	Rb	10−5	5.05	1550
9	Rb	6−3	5.01	900

For this purpose, we must have the molecular diameter (σ) for each of the LJ ($n-m$) pair potentials. We calculated these values and also isolated well-depth potential (ϵ) for rubidium for some n and m, using the experimental second virial coefficients. These values have been collected in Table 2. We then have calculated the values for d_{eff} and ϵ_{eff} using eqs 8 and 17. These values are summarized in Table 3. We found that all of the calculated structure factors do not have any agreement with the experimental data and, hence, these potentials cannot describe the structure of alkali metals by selecting any values for their parameters in our examined range. Figure 5 shows some of these typical results for $T = 2000$ K, at which temperature its state is near the critical point. We chose this state because a simple potential without any oscillating component may be appropriate in this region (note that the LJ ($n-m$) model does not have any

TABLE 3: DCF Parameters for Rubidium Using LJ ($n-m$) Pair Potentials for Some Thermodynamic States

No.	substance	temperature, T (K)	ρ (Å^{-3})	$S(0)$	LJ potential ($n-m$)	σ (Å)	ϵ_{eff}/k (K)	d/σ
1	Rb	2000	0.00379	3.51	12−6	5.20	1644.7	1.008
2	Rb	1400	0.00684	0.40	12−6	5.20	832.7	1.046
3	Rb	350	0.01028	0.02	12−6	5.20	3357.9	1.065
4	Rb	2000	0.00379	3.51	6−3	5.01	86.5	0.769
6	Rb	1400	0.00684	0.4	6−3	5.01		
6	Rb	350	0.01028	0.02	6−3	5.01		
5	Rb	2000	0.00379	3.51	12−5	5.05	1285.6	0.996
6	Rb	2000	0.00379	3.51	12−4	5.05	764.0	0.975
7	Rb	2000	0.00379	3.51	12−3	5.02	244.6	0.911
8	Rb	2000	0.00379	3.51	10−5	5.05	1095.6	0.991
9	Rb	2000	0.00379	3.51	8−6	5.15	1284.2	0.998
10	Rb	2000	0.00379	3.51	11−6	5.05	1472.4	1.004
11	Rb	2000	0.00379	3.51	10−6	5.11	1447.8	1.004
12	Cs	1673	0.00345	0.86	6−3[b]	4.65	7100	1.242[a]
13	Cs	773	0.00711	0.07	6−3[b]	4.39	11050	1.175[a]

[a] Calculated from eq 8. [b] From ref 2.

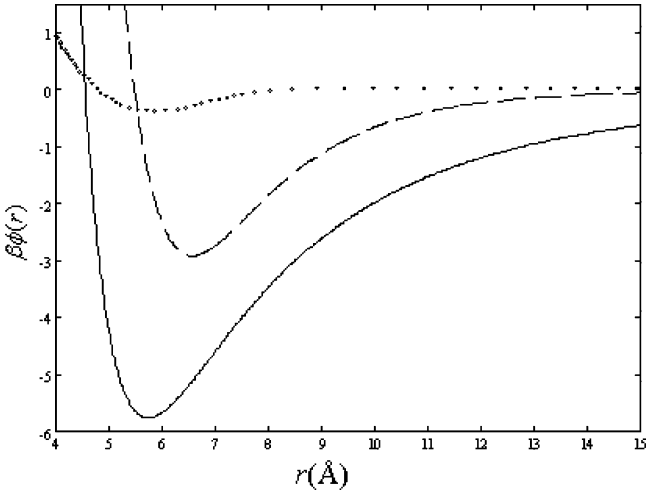

Figure 6. Comparison of effective pair potentials ((●) MHNC (from ref 6), (—) LJ (6−3) (from ref 2), and (− −) exp-6 (from ref 1)) for cesium at $T = 1373$ K and $\rho = 1.21$ g/cm^3.

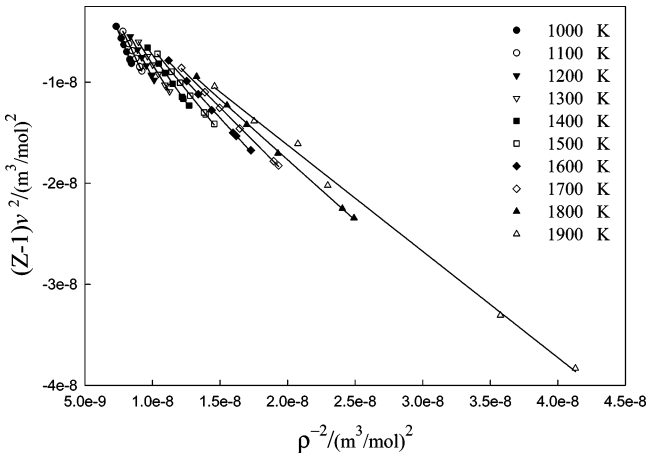

Figure 7. Isotherms of $(Z - 1)v^2$ versus ρ^{-2} for cesium at 400−1950 K (shown for 1000−1900 K only), using the pressure−volume−temperature ($p-v-T$) data of ref 23.

bumping). Figure 6 shows the MHNC, LJ (6−3), and exp-6 potentials (from refs 6, 2, and 1, respectively) for cesium at $T = 1373$ K and $\rho = 1.21$ g/cm^3. The difference between the three potentials clearly is very noticeable. In this way, we can say, at least for these thermodynamic states, that the experimental results show that the LJ (6−3) and exp-6 models are insufficient to present the effective pair potential for cesium (note that the pair potential for this thermodynamic state may be presented with a potential without oscillations); therefore, we do not expect that these potentials would be able to predict $S(k)$ at high densities, where the oscillatory component of the potential is so important.

To confirm our conclusion, we have shown that the isotherms of $(Z - 1)v^2$ are not very sensitive to density functionality; for example, it is linear versus ρ for isotherms at 350−1700 K, versus $1/\rho^2$ for isotherms at 350−1950 K, and versus $1/\rho^3$ for isotherms at 350−1750 K for cesium. This linearity is even observed for plots involving $1/\rho^{10}$ for low-temperature isotherms. Some of these results have been shown in Figure 7. In accordance with these observations, one can say that the $p-v-T$ data of the alkali metals in the LIR-type EOS are not very sensitive to the type of potentials. In conclusion, we cannot use this method (LIR derivation) to find the effective pair potential for alkali metals. Of course, to get $p-v-T$ data at high densities or high pressures, perhaps such insensitivity is fortunate.

4. Conclusion

We have used a new model for the direct correlation function (DCF) and the experimental effective pair potentials to predict the low-k behavior of the structure factor $S(k)$ of rubidium and cesium. The agreement for densities more than the metal−nonmetal transition (M−NMT) densities were very good. Note that, for these states, some bumping exists in the long-range limit of potentials, and we know that the long-range repulsion also has an important role in the prediction of $S(k)$ at low k. Also, we may conclude that the effective pair potential with no bumping is not appropriate to predict the $S(k)$, at least for the low-k values in our examined range. The results of this article and previous works[13,17] show that the nonlinear form of the DCF tail is appropriate, even for fluids with long-range oscillating potentials, in addition to simple LJ liquids. Furthermore, we have shown that any LJ ($n-m$) pair potentials are not reliable to describe the behavior of the structure factor of alkali metals, for the selection of any values for their parameters, because the sensitivity of $S(k)$ to the long-range potential at low k is very high. Again, we confirm that these potential may be applied to predict the pressure−volume−temperature ($p-v-T$) behavior in the LIR form; however, their failure to predict $S(k)$ may be related to the high sensitivity of $S(k)$ at low k to the oscillatory repulsion at the long-range limit.

Acknowledgment. We acknowledge the Isfahan University of Technology Research Councils for their financial support. This work has been supported by Grant No. 1CHA 802.

References and Notes

(1) Ghatee, M. H.; Shams-Abadi, H. *J. Phys. Chem. B* **2001**, *105*, 702.
(2) Ghatee, M. H.; Bahadori, M. *J. Phys. Chem. B* **2001**, *105*, 11256.
(3) Kahl, G.; Hafner, J. *Phys. Rev. A* **1984**, *29*, 3310.
(4) Mansoori, G. A.; Jedrzejek, C.; Shah, N. H.; Blander, M. *Chemical Metallurgy—A Tribute to Carl Wagner*; Gokcen, N. A., ed.; The Metallurgical Society of AIME: Warrendale, PA, 1981; pp 233−240.
(5) Evans, R.; Slukin, T. J. *J. Phys. C: Solid State Phys.* **1981**, *14*, 3137.
(6) Munejiri, S.; Shimojo, F.; Hoshino, K.; Watabe, M. *J. Phys. C: Condens. Matter* **1997**, *9*, 3303.
(7) Munejiri, S.; Shimojo, F.; Hoshino, K.; Watabe, M. *J. Non-Cryst. Solids* **1996**, *205*, 278.
(8) McLaughlin, I. L.; Young, W. H. *J. Phys. F: Met. Phys.* **1982**, *12*, 95.
(9) Matsuda, N.; Hoshino, K.; Watabe, M. *J. Chem. Phys.* **1990**, *93* (10), 7350.
(10) Pini, D.; Parola, A.; Reatto, L. *Mol. Phys.* **2002**, *100* (10), 1507.
(11) Weeks, J. D.; Chandler, D.; Andersen, H. C. *J. Chem. Phys.* **1971**, *54*, 5237.
(12) Evans, R.; Slukin, T. J. *J. Phys. C: Solid State Phys.* **1981**, *14*, 2569.
(13) Keshavarzi, E.; Nikoo-fard, H.; Rostami, A. A. *J. Phys. Soc. Jpn.* **2003**, *72*, 1983.
(14) Evans, R.; Slukin, T. J. *J. Phys. C: Solid State Phys.* **1982**, *14*, 1121.
(15) Vliegenthart, G. A.; Lekkerkerker, H. N. *J. Chem. Phys.* **2000**, *112*, 5364.
(16) Verlet, L. *Phys. Rev.* **1968**, *165*, 201.
(17) Keshavarzi, E.; Parsafar, G. A. *J. Phys. Soc. Jpn.* **2001**, *70*, 1979.
(18) Croxton, C. A. *Introduction to Liquid State Physics*; Wiley: New York, 1978.
(19) Parsafar, G. A.; Mason, E. A. *J. Phys. Chem.* **1993**, *97*, 9048.
(20) Keshavarzi, E.; Parsafar, G. A. *J. Phys. Chem. B* **1999**, *103*, 6584.
(21) Bratkovsky, A. M.; Vaks, V. G.; Kravchuk, S. P.; Trefilov, A. V. *J. Phys. F: Met. Phys.* **1982**, *12*, 1293.
(22) Franz, G.; Freyland, W.; Gläser, W.; Hensel, F.; Schneider, E. *J. Phys. Coll. Suppl.* **1980**, *41*, 194.
(23) Vargaftik, N. B.; Gelman, E. B.; Kozhevnikov, V. F.; Naursakov, S. P. *Int. J. Thermophys.* **1990**, *11* (3), 467.